**Online Data Supplyment**

# RAGE induced ILC2 expansion in Acute Lung Injury due to Haemorrhagic Shock

Kai Zhang[1,2§], Yue Jin[1§], Dengming Lai[2,3], Jieyan Wang[2], Yang Wang[1], Xiaoliang Wu[1], Melanie J. Scott[2], Yuehua Li[2,4], Jinchao Hou[1], Timothy R. Billiar[2,5], Mark A. Wilson[2,4], Qiang Shu[3], Xiangming Fang[1,*], Jie Fan[2,4,5,*]

## Supplementary Materials and Methods

### Mice

C57BL/6J wild-type (WT) mice, C57BL/6J CD45.1 mice (B6.SJL-Ptprca Pepcb/BoyJ) and C57BL/6-*Rag1*$^{-/-}$ (B6.129S7-Rag1tm1Mom/J) mice were purchased from Jackson Laboratories. Inducible *Hmgb1*$^{-/-}$ mice and *Hmgb1*$^{flox/flox}$ on a C57BL/6 background,[1] C57BL/6-*Rage*$^{-/-}$ mice, C57BL/6-*Tlr4*$^{-/-}$ mice, and C57BL/6-*Tlr9*$^{-/-}$ mice were bred and maintained under specific pathogen-free conditions at the University of Pittsburgh School of Medicine Animal Facility. All mice were carried out using 8-10 week-old according to the guidelines of the Institutional Animal Care and Use Committees (IACUC) of the University of Pittsburgh and VA Pittsburgh Healthcare System.

### Recombinant HMGB1 treatment of mice

Mice were treated with recombinant HMGB1 (rHMGB1 2 mg/kg, R&D Systems, Minneapolis, MN, US) or phosphate buffered saline (PBS) as control in a volume of 50 µl injected intratracheally (i.t.) 24h prior to the measurements.

### Isolation of cells from human peripheral blood

Peripheral blood samples were obtained from healthy donors or patients at 24 hours after the diagnosis of HS, with a standard collection system and EDTA as anticoagulant. 1 ml whole



Zhang K, *et al. Thorax* 2024; 75:209–219. doi: 10.1136/thoraxjnl-2019-213613

blood were lysed using ACK lysis buffer (eBioscience, San Diego, CA, US) and single-cell suspensions were collected for further analysis.

**Isolation of cells from mouse tissue**

Bone marrow (BM) cells were collected from femora and tibiae. Spleens and mediastinal lymph nodes (MLNs) were dissociated into single cell suspensions using ground glass slides. Isolation of cells from lung tissue was done as described previously.[2] Briefly, after whole lungs were removed and cut into small fragments, tissue was digested with Liberase TM (50 µg/ml. Roche, Mannheim, Germany) and DNase I (1 µg/ml, Roche) for 60 min at 37°C with shaking at 100 rpm and red blood cells were lysed with ACK buffer (eBioscience). Isolation of cells from intestines was performed as described previously.[2, 3] Briefly, small intestines were removed and flushed with two washes of 10 ml of cold PBS. Intestines were cut into small pieces and digested with 2 mg/ml collagenase D (Roche) in PBS for 45-60 min at 37°C with vortexing every 10 min. Mononuclear cells from epididymal white adipose tissues were isolated as previously described.[2, 4] The adipose tissue was minced with scissors and then digested with 1 mg/mL collagenase type II (Sigma-Aldrich) at 37°C for 60 min with vortexing every 10 min. All samples were pressed through 70-µm cell strainers and washed with cold PBS twice, and any remaining red blood cells were lysed using ACK lysis buffer (eBioscience). Single-cell suspensions from all tissues were collected for further analysis.

**Flow cytometric analysis and sorting**

Single-cell suspensions were prepared and incubated with purified anti-CD16/32(clone 93, eBioscience) for 20 min on ice to block Fc receptors before staining. For mouse studies, the following antibodies were used in the experiments: fluorochrome-labelled monoclonal antibodies against CD3 (17A2, eBioscience), CD3e (145-2C11, eBioscience), CD4 (RM4-5,



Zhang K, *et al. Thorax* 2024; 75:209–219. doi: 10.1136/thoraxjnl-2019-213613

eBioscience), CD5 (53-7.3, eBioscience), CD8a (53-6.7, eBioscience), CD11b (M1/70, eBioscience), CD11c (N418, eBioscience), CD19 (eBio1D3, eBioscience), CD25 (PC61, eBioscience), CD45 (30-F11, BD Biosciences, San Jose, CA, US), B220 (RA3-6B2, eBioscience, US), Gr-1 (RB6-8C5, eBioscience), TCRβ (N57-597, eBioscience), γδTCR (eBioGL3, eBioscience), FcεR1 (MAR-1, eBioscience), NK1.1 (PK136, eBioscience, US), Ter-119 (TER-119, eBioscience), F4/80 (BM8, eBioscience), KLRG1 (2F1, eBioscience), CD127 (SB/199, BD Biosciences), CD90.2 (53-2.1, eBioscience), Sca-1 (D7, BD Biosciences), ST2 (DJ8, MD Biosciences, Oakdale, MN, US), Siglec-F (E50-2440, BD Biosciences), RAGE (A-9, Santa Cruz, Dallas, TX, US), CD45.1 ( A20, BD Biosciences), CD45.2 (104, BD Biosciences), HMGB1 (3E8, BioLegend, San Diego, CA, US), Gata-3 (TWAJ, BD Biosciences), IL-4 (11B11, eBioscience), IL-5 (TRFK5, eBioscience), IL-9 (D9302C12, eBioscience), IL-13 (eBio13A, eBioscience), BCL-2 (BCL/10C4, Biolegend), Bax (6A7 eBioscience), and Ki-67 (B56, BD Biosciences). lineage-negative gating included markers for CD3, CD4, CD5, CD8a, CD11b, CD11c, CD19, B220, Gr-1, TCRβ, γδTCR, F4/80, Ter-119, FcεR1 and NK1.1. Details of immunostaining and gating strategies for mouse ILC2s are described in the supplemental figure 8.

For human studies, single-cells were stained with fluorochrome-labelled monoclonal antibodies against: CD2 (RPA-2.10, BD Biosciences), CD3 (OKT3, BD Biosciences), CD4 (OKT4, BD Biosciences), CD14 (61D3, BD Biosciences), CD16 (CB16, BD Biosciences), CD19 (HIB19, BD Biosciences), CD45 (HI30, BD Biosciences), CD56 (B159, BD Biosciences), CD66 (B1.1/CD66, BD Biosciences), CD235a (HIR2, BD Biosciences), Nkp44 (p44-8, BD Biosciences), CRTH2 (BM16, BD Biosciences), CD127 (eBioRDR5, BD Biosciences), ST2 (B4E6, MD Biosciences), RAGE (161205, R&D Systems), IL-5 (TRFK5, BD Biosciences), IL-13 (JES10-5A2, BD Biosciences). lineage-negative gating included markers for CD2, CD3, CD4, CD14, CD16, CD19, CD56, CD235a. Details of

immunostaining and gating strategies for human ILC2s are described in the supplemental figure 9.

For measurement of intracellular cytokine expression, cells were isolated and incubated with 500 ng/ml ionomycin (Sigma-Aldrich), 50 ng/ml phorbol 12-myristate 13-acetate (Sigma-Aldrich) and 10 μg/ml brefeldin A (Sigma-Aldrich) in DMEM media (Gibco, Waltham, MA, US) with 10% fetal bovine serum (FBS) (Denville Scientific, Holliston, MA, US) for 4 h at 37°C. Cells were then re-suspended and stained for surface antigens and subsequently fixed and permeabilized with a commercial kit (intracellular fixation and permeabilization buffer set, eBioscience) according to the manufacturer's recommendations then incubated with specific antibodies to IL-4, IL-5, IL-9, and IL-13.

Intranuclear protein staining was performed using the Foxp3 staining kit (eBioscience) according to the manufacturer's instructions. For detection of apoptosis, cells were prepared and stained with annexin V and 7-amino-actinomycin D (7-AAD, PE Annexin V Apoptosis Detection Kit I, BD Biosciences) according to the manufacturer's instructions. For measurement of mitochondrial function, cells were isolated directly *ex vivo* and stained with MitoTracker® Deep Red FM (Invitrogen, Eugene, OR, US) and MitoStatus Red (BD Biosciences) according to the manufacturer's instructions. All samples were acquired on a BD LSRII flow cytometer (BD Bioscences) and analyzed with FlowJo software (v10.0, Tree Star)

For mouse ILC2 sorting, cells were stained with lineage cocktail Abs (CD3, CD4, CD5, CD8a, CD11b, CD11c, CD19, B220, Gr-1, TCRβ, γδTCR, F4/80, Ter-119, FcεR1 and NK1.1); anti-CD45 Ab; anti-ST2 Ab; and anti-CD90.2 Ab, at 4 °C for 30 min. ILC2s were defined as $CD45^+$ $Lin^-$ $CD90.2^+$ $ST2^+$ and sorted by FACS Aria (BD Biosciences). The average purity of ILC2s was >95%.

**In Vivo Depletion of ILC2s**

For depletion of ILC2s in mice anti-Thy1.2 monoclonal Ab (30H12, BioXCell, West Lebanon, NH) was used. *Rag1*$^{-/-}$ mice were injected i.p. every 3 days at a dose of 250μg/mouse starting on day 0 and ending on day 7.[5]

**Adoptive transfers of lung ILC2s**

Donor mice were treated intranasally on days 1, 3 and 5 with 1μg recombinant murine IL-33 (BioLegend, San Diego, CA) for ILC2 population expansion. On day 7, viable $CD45^+$ $Lin^-$ $CD90.2^+$ $ST2^+$ cells were purified and $5\times 10^4$ cells were transferred via tail vein injections.

**Immunoblotting**

Western blot assays were performed using whole cell lysates from lung tissue. Membranes were incubated with anti-HMGB1 antibody (Abcam, Cambridge, MA, US) at 4°C overnight. Protein bands were visualized using the Odyssey System (LI-COR Biosciences, Lincoln, NE, US).

**Cytokine ELISA**

Plasma samples from HS patients were collected and cytokine protein levels of IL-4 (eBioscience), IL-5 (eBioscience), IL-9 (eBioscience), IL-13 (eBioscience) and HMGB1 (CUSABIO, Houston, TX, US) were measured using the human ELISA kits according to the manufacturers' instructions.

Plasma cytokine protein levels of IL-4 (eBioscience), IL-5 (eBioscience), IL-9 (Abcam), IL-13 (eBioscience) and HMGB1 (IBL International) from mice samples were measured using the Mouse ELISA kits according to the manufacturers' instructions.



Zhang K, *et al. Thorax* 2024; 75:209–219. doi: 10.1136/thoraxjnl-2019-213613

**Lung histology and lung injury scoring**

Histology of lung sections from each mouse was examined after staining with hematoxylin and eosin. The levels of lung injury were evaluated according to the semi-quantitative lung injury scoring system as described previously.[6]



Zhang K, *et al. Thorax* 2024; 75:209–219. doi: 10.1136/thoraxjnl-2019-213613

## References

1. Vogel S, Bodenstein R, Chen Q *et al*. Platelet-derived HMGB1 is a critical mediator of thrombosis. *J Clin Invest* 2015; 125: 4638-54.

2. Moro K, Ealey KN, Kabata H, Koyasu S. Isolation and analysis of group 2 innate lymphoid cells in mice. *Nat Protoc* 2015; 10: 792-806.

3. Hoyler T, Klose CS, Souabni A *et al*. The transcription factor GATA-3 controls cell fate and maintenance of type 2 innate lymphoid cells. *Immunity* 2012; 37: 634-48.

4. Moro K, Yamada T, Tanabe M *et al*. Innate production of T(H)2 cytokines by adipose tissue-associated c-Kit(+)Sca-1(+) lymphoid cells. *Nature* 2010; 463: 540-4.

5. Monticelli LA, Sonnenberg GF, Abt MC *et al*. Innate lymphoid cells promote lung-tissue homeostasis after infection with influenza virus. *Nat Immunol* 2011; 12: 1045-54.

6. Belperio JA, Keane MP, Burdick MD *et al*. Critical role for CXCR2 and CXCR2 ligands during the pathogenesis of ventilator-induced lung injury. *J Clin Invest* 2002; 110: 1703-16.

Table S1. Characteristics of hemorrhagic shock patients and healthy controls.

| | Hemorrhagic shock (n=34) | Healthy controls (n=33) | P value |
|---|---|---|---|
| Age (yr) | 57.32±2.52 | 51.45±2.07 | 0.08 |
| Male sex (%) | 25 (73.53) | 18 (54.55) | 0.11 |
| ISS | 16.00 (16.00-25.00) | | |
| APACHE II score | 14.50 (11.00-18.00) | | |
| SOFA score | 7.00 (5.00-10.00) | | |
| Blood lactate acid (mmol/L) | 2.65 (2.03-6.15) | | |
| ICU length of stay (days) | 4.5 (2-11) | | |
| Hospital length of stay (days) | 15 (11.75-25.25) | | |

Data are expressed as the mean ± SEM, mediean (interquartile rage) or number (%) where applicable. Student *t* test was used to compare differences in continuous variables between two groups. Differences in categorical data were compared using Chi-Squared test.
ISS= Injury severity score; APACHE II = Acute Physiology and Chronic Health Evaluation II; SOFA = Sequential Organ Failure Assessment; ICU = Intensive Care Unit.



Zhang K, *et al. Thorax* 2024; 75:209–219. doi: 10.1136/thoraxjnl-2019-213613

**Figure Legends**

**online supplementary figure 1. Flow cytometric detection of intracellular cytokine IL-5 and IL-13 production in human blood ILC2s.**

(A) Representative flow cytometry blots and graph showing percentages of IL-5$^+$ ILC2s (CD45$^+$ Lin$^-$ NKp44$^-$ CD127$^+$ CRTH2$^+$ ST2$^+$) in HS patients and healthy controls. (B) Representative flow cytometry blots and graph showing percentages of IL-13$^+$ ILC2s in HS patients and healthy controls. All results are shown as mean ± SD. Date were analyzed by Mann-Whitney test.

**online supplementary figure 2. ILC2s are increased in the lungs of mice with HS.**

(A) Representative flow cytometry plots showing percentages of ILC2s (CD45$^+$ Lin$^-$ CD90.2$^+$ ST2$^+$) within the CD45$^+$ Lin$^-$ cell populations and (B) graphs showing percentages and absolute numbers of ILC2s in the lungs of WT mice at 0, 6, 12, 24, 36, 48, and 72h after HS or sham surgery. All results are shown as mean ± SD. Date were analyzed by Mann-Whitney test.

**online supplementary figure 3. HS-induced HMGB1 expression among pulmonary cell populations.**

(A) Flow cytometric analysis and (B) mean fluorescence intensity (MFI) levels of HMGB1 expression in lung epithelial cells (CD45$^-$ CD326$^+$), eosinophils (CD45$^+$ Gr-1$^-$ CD11b$^+$ Siglec-F$^+$), macrophages (CD45$^+$ F4/80$^+$) and neutrophils (CD45$^+$ Gr-1$^+$) at 24h after HS or sham. All results are shown as mean ± SD. Date were analyzed by Kruskal-Wallis test.

**online supplementary figure 4. HMGB1-RAGE regulates ILC2 differentiation after HS.**

(A) Representative flow cytometric analysis and MFI levels of GATA3 expression in lung ILC2s (CD45$^+$ Lin$^-$ CD90.2$^+$ CD25$^+$ CD127$^+$ KLRG1$^+$) from WT, *Hmgb1*$^{-/-}$ and *Rage*$^{-/-}$ mice at 24h after HS or sham surgery. (B) Flow cytometric analysis plots and graphs showing percentages of immature ILC2s (CD45$^+$ Lin$^-$ CD90.2$^+$ CD127$^+$ GATA3$^+$ KLRG1$^-$) pre-gated

on $CD45^+ Lin^- CD90.2^+ CD127^+$ in the lungs of the same experimental mice. All results are shown as mean ± SD. Date were analyzed by Mann-Whitney test.

**online supplementary figure 5. Characterization of cytokine expression and secretion from lung ILC2s after rHMGB1 treatment.**

(A-C) Representative flow cytometry blots and graph showing percentages of (A) IL-$5^+$ ILC2s ($CD45^+ Lin^- CD90.2^+ ST2^+$), (B) IL-$9^+$ ILC2s and (C) IL-$13^+$ ILC2s in the lungs of WT mice at 24h after treatment with i.t. instilled rHMGB1 (2 mg/kg) or PBS. (D) ELISA analysis of plasma IL-5, IL-9 and IL-13 concentrations in WT mice at 24h after treatment with i.t. instilled rHMGB1 (2 mg/kg) or PBS. All results are shown as mean ± SD. Date were analyzed by Mann-Whitney test.

**online supplementary figure 6. IlC2-depletion attenuated rHMGB1-induced type 2 inflammation in the lungs.**

(A) Flow cytometry showing percentages of ILC2s ($CD45^+ Lin^- CD90.2^+ ST2^+$) from isotype and αThy1.2-treated *Rag1*$^{-/-}$ mice at 24h after given i.t. rHMGB1 gated on $CD45^+ Lin^-$ populations. (B) ELISA analysis of plasma IL-5, IL-9 and IL-13 concentrations from isotype and αThy1.2-treated *Rag1*$^{-/-}$ mice at 24h after given i.t. rHMGB1 gated on $CD45^+ Lin^-$ populations. All results are shown as mean ± SD. Date were analyzed by Mann-Whitney test.

**online supplementary figure 7. Adoptive transfer experiment recovered ILC2s in *Hmgb1*$^{-/-}$ and *Rage*$^{-/-}$ mice.**

(A) Flow cytometry blots showing percentages of ILC2s ($CD45^+ Lin^- CD90.2^+ ST2^+$) within the $CD45^+ Lin^-$ cell populations and graphs showing absolute numbers of ILC2s in the lungs at 24h after HS in *Hmgb1*$^{-/-}$ mice transferred with ILC2s ($5\times10^4$ cells/mouse) isolated from WT mice. (B) Flow cytometry blots showing percentages of ILC2s within the $CD45^+ Lin^-$ cell populations and graphs showing absolute numbers of ILC2s in the lungs at 24h after HS in *Rage*$^{-/-}$ mice transferred with ILC2s ($5\times10^4$ cells/mouse) isolated from WT mice. (C)

ILC2s were purified from CD45.1 mice and transferred into *Rage*$^{-/-}$ (CD45.2) mice. Donor (CD45.1) and host (CD45.2) ILC2s in lung, mLNs and spleen were analyzed by flow cytometric. All results are shown as mean ± SD. Date were analyzed by Mann-Whitney test.

**online supplementary figure 8. Gating strategy for the identification of ILC2s in mice.**

(A) Representative flow cytometry plots show the gating strategy for characterization of ILC2s in mice lung tissue. A lymphocyte gate was drawn (according to FSC and SSC properties) and doublets were excluded. $CD45^+$ $Lin^-$ cells were further electronically gated into $CD90.2^+$ $ST2^+$ $CD127^+$ $CD25^+$ $Sca\text{-}1^+$ $KLRG1^+$. Lin markers include CD3, CD4, CD5, CD8a, CD11b, CD11c, CD19, B220, Gr-1, TCRβ, γδTCR, F4/80, Ter-119, FcεR1 and NK1.1. (B) Isotype and FMO controls of lineage negative gate for murine ILC2s.

**online supplementary figure 9. Gating strategy for the identification of ILC2s in human.**

(A) Representative flow cytometry plots show the gating strategy for characterization of ILC2s in human blood. A lymphocyte gate was drawn (according to FSC and SSC properties) and doublets were excluded. $CD45^+$ $Lin^-$ leucocytes were further gated into $NKp44^-$ $CD127^+$ $CRTH2^+$ $ST2^+$. Lin markers include CD2, CD3, CD4, CD14, CD16, CD19, CD56 and CD235a. (B) Isotype and FMO controls of lineage negative gate for human ILC2s.

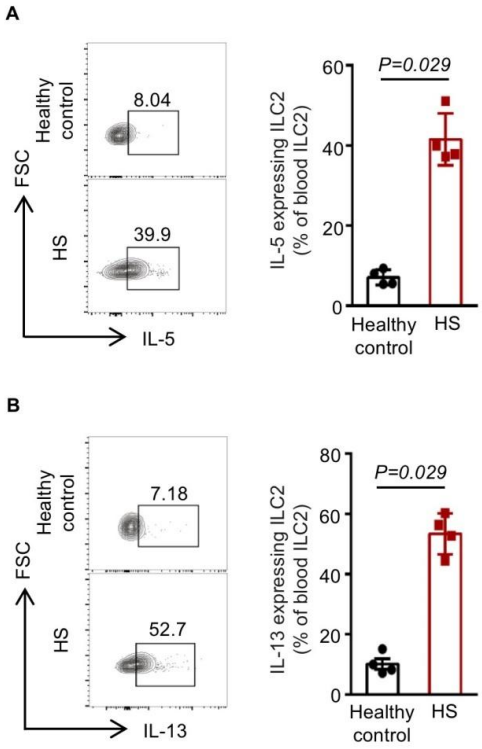


online supplementary figure 1. Flow cytometric detection of intracellular cytokine IL-5 and IL-13 production in human blood ILC2s.

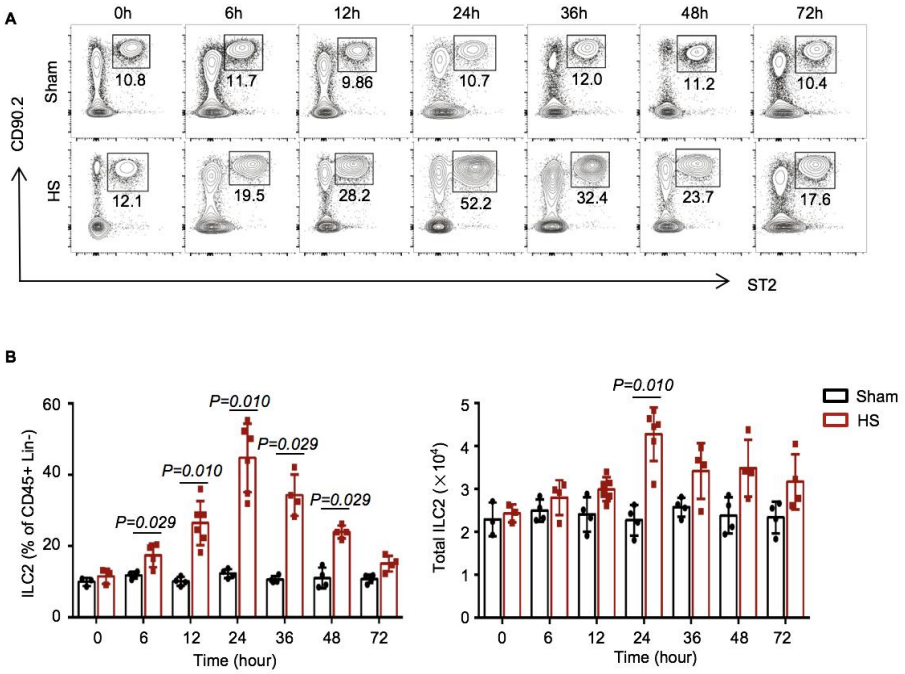


online supplementary figure 2. ILC2s are increased in the lungs of mice with HS.

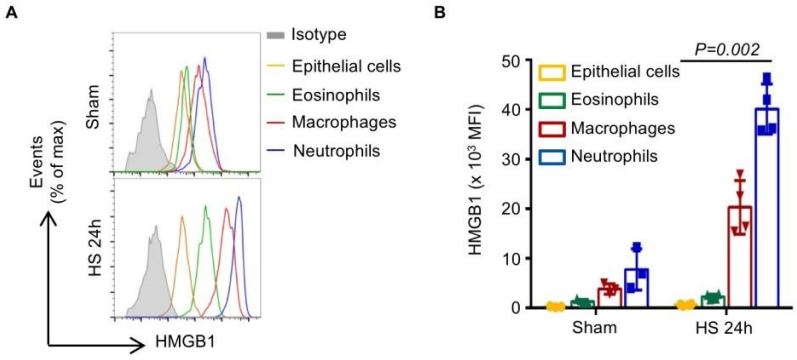


online supplementary figure 3. HS-induced HMGB1 expression among pulmonary cell populations.

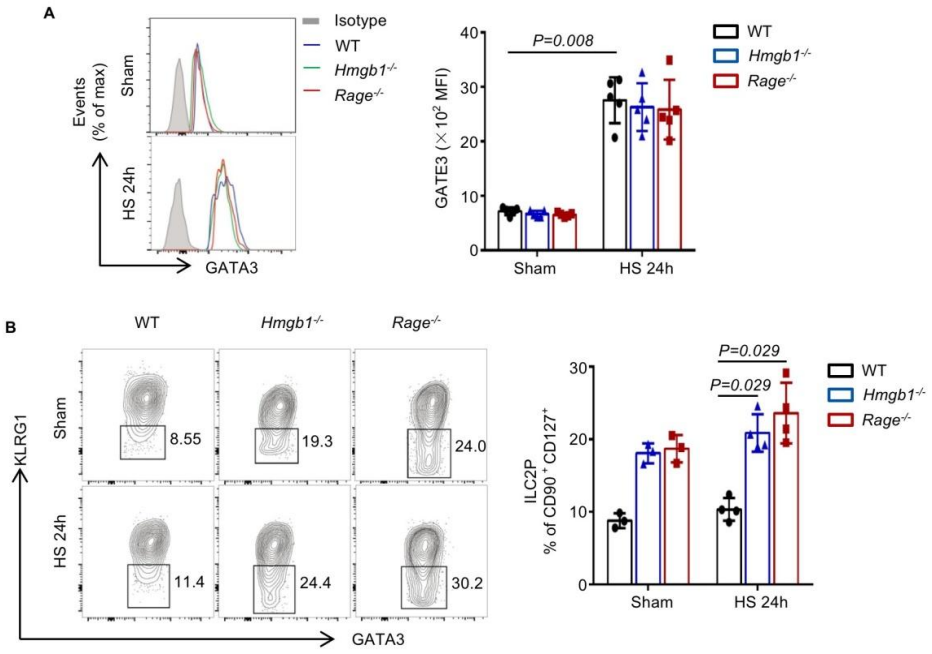


online supplementary figure 4. HMGB1-RAGE regulates ILC2 differentiation after HS.

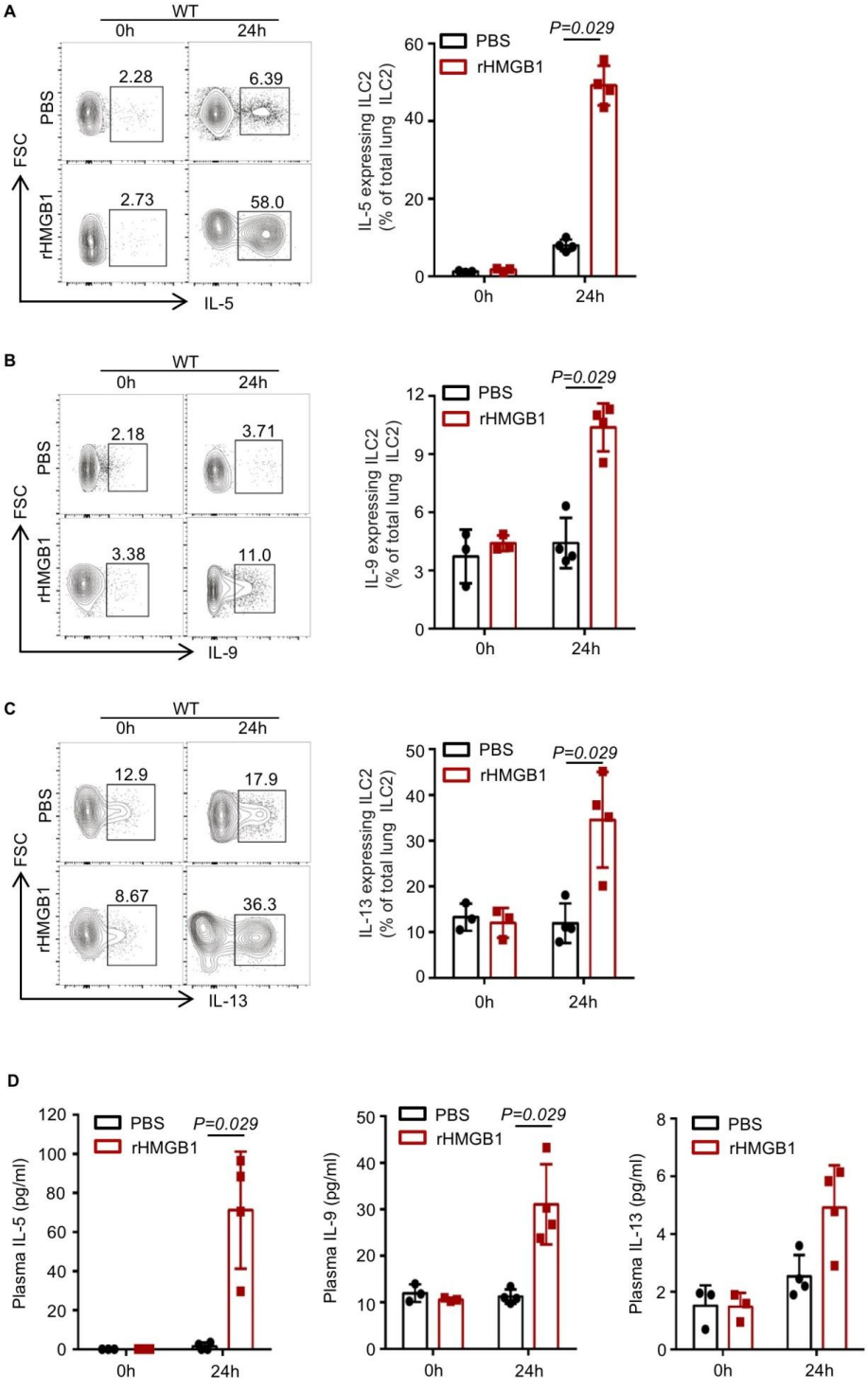


online supplementary figure 5. Characterization of cytokine expression and secretion from lung ILC2s after rHMGB1 treatment.

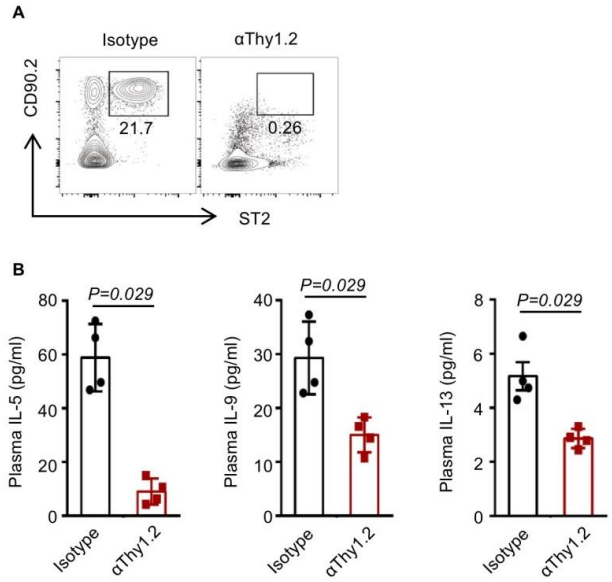


online supplementary figure 6. IlC2-depletion attenuated rHMGB1-induced type 2 inflammation in the lungs.

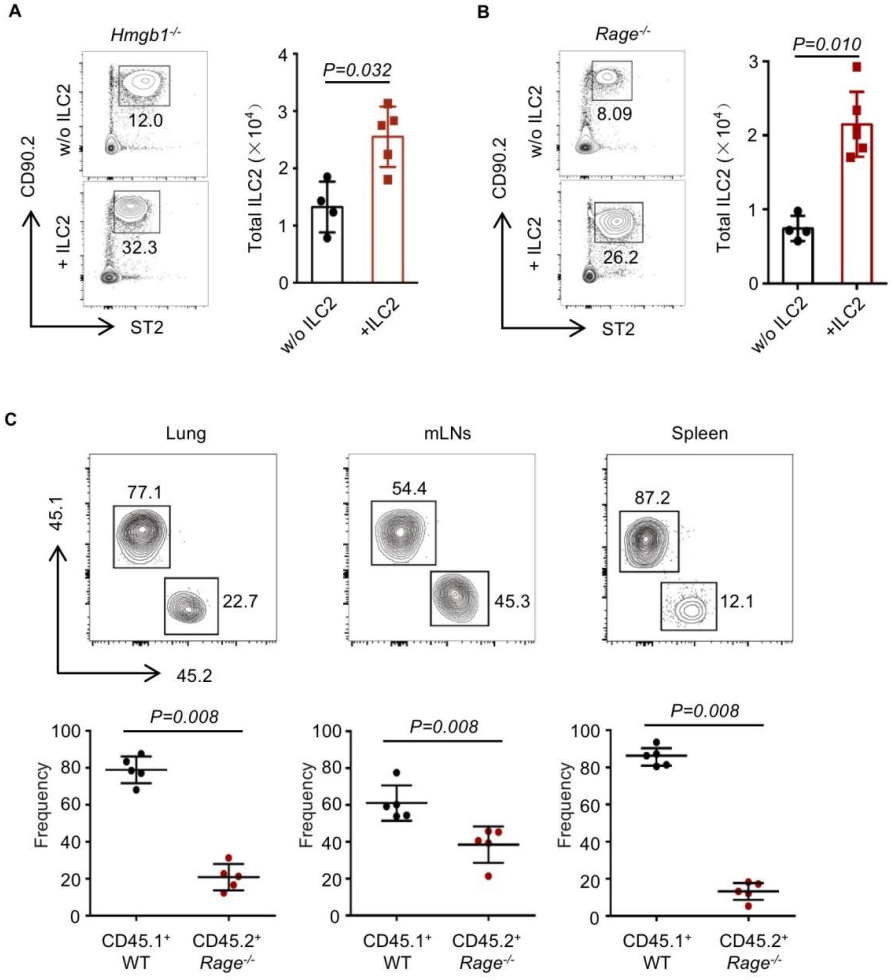


online supplementary figure 7. Adoptive transfer experiment recovered ILC2s in *Hmgb1*$^{-/-}$ and *Rage*$^{-/-}$ mice.

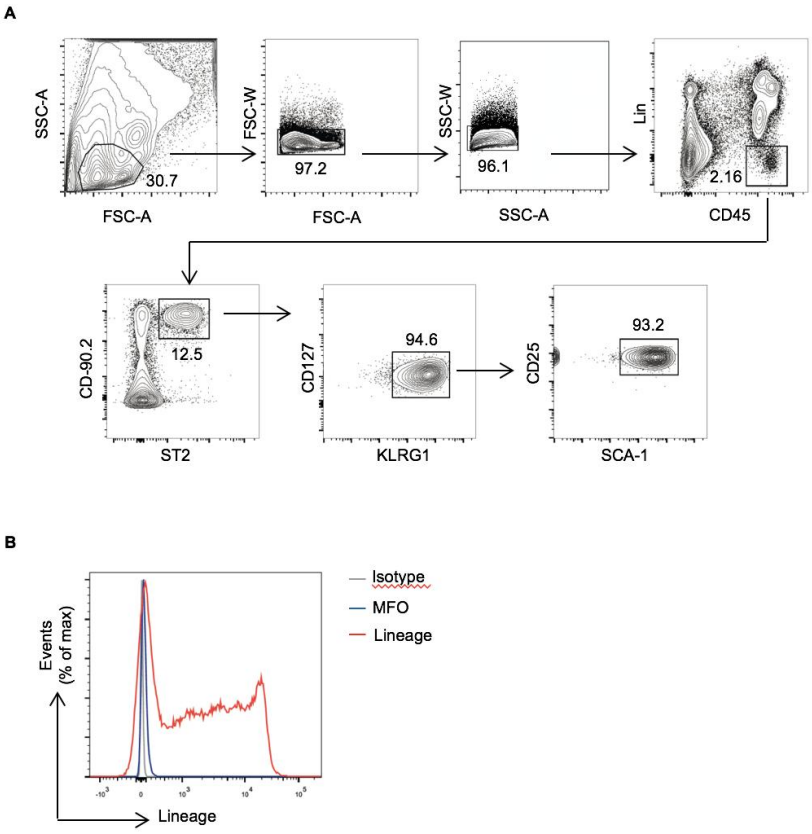


online supplementary figure 8. Gating strategy for the identification of ILC2s in mice.

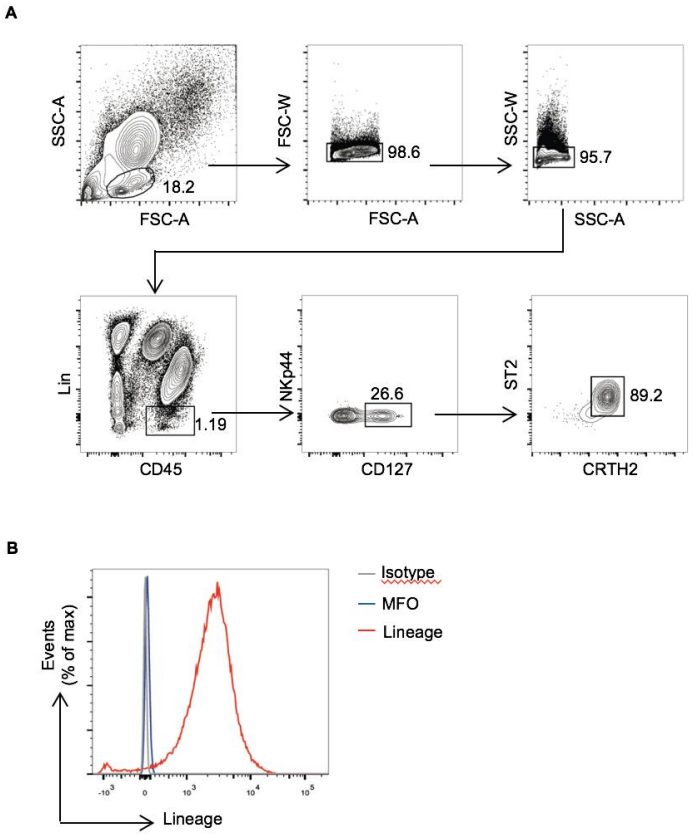


online supplementary figure 9. Gating strategy for the identification of ILC2s in human.